DEPARTMENT OF DEFENCE
DEFENCE SCIENCE & TECHNOLOGY ORGANISATION
DSTO

A Comparison of Recursive Style Angle-only Target Motion Analysis Algorithms

Sanjeev Arulampalam

DSTO-TR-0917

A Comparison of Recursive Style Angle-only Target Motion Analysis Algorithms

Sanjeev Arulampalam

Surveillance Systems Division
Electronics and Surveillance Research Laboratory

DSTO–TR–0917

ABSTRACT

This report presents a comparison of existing angle-only target motion analysis algorithms which have applications in tracking under jamming conditions. Though a number of different algorithms have been proposed for this problem, the particular emphasis in this report is recursive style algorithms which are more suited to airborne applications. In particular, six algorithms are considered, which are derivatives of either the standard or the extended Kalman filter. Four of these algorithms are single-filter trackers while the other two are based on weighted sum of multiple filter outputs. Simulation results are presented to verify the claimed properties of these algorithms

Authors

Sanjeev Arulampalam
Surveillance Systems Division

Sanjeev Arulampalam received the B.Sc degree in Mathematical Sciences and the B.E degree with first class honours in Electrical and Electronic Engineering from the University of Adelaide in 1991 and 1992, respectively. In 1992 he joined the staff of Computer Sciences of Australia (CSA) where he worked as a Software Engineer in the Safety Critical Software Systems group. At CSA he was responsible for undertaking a hazard analysis on a computerised train control system. In 1993, he won a Telstra Postgraduate Fellowship award to work toward a Ph.D degree in Electrical and Electronic Engineering at the University of Melbourne, which he completed in 1997. His doctoral dissertation was "Performance Analysis of Hidden Markov Model based Tracking Algorithms".

Upon completion of his postgraduate studies, Dr Arulampalam joined the Defence Science and Technology Organisation in 1998 as a Research Scientist in the Surveillance Systems Division. Since then he has worked on tender evaluation of the AEW&C contracts, and is currently involved in angle-only target motion analysis research for the F/A-18 project. His research interests include estimation theory, signal processing, and target motion analysis.

Contents

Appendices

Figures

1 Introduction

The problem of angle-only Target Motion Analysis (TMA) arises in a variety of important practical applications including sonar and radar. The fundamental objective of angle-only TMA, also known as passive ranging, is to track the kinematics (position and velocity) of a moving target using noise corrupted angle measurements only. In the case of autonomous passive ranging (single observer only), which we shall consider in this report, the observation platform needs to move in order to estimate the range of the target. The application of interest for our study is the tracking from an airborne platform, of an airborne target for which range information is not available, for example, as a result of noise jamming by the target. In such situations, the tracker needs to be able to maintain track, and estimate the range of the jammer, using angle measurements only.

Various forms of solutions/algorithms have been proposed for the angle-only TMA problem [1, 2, 3, 4, 10], which mainly fall into two categories: batch processing type, and recursive type. The batch processing type involves delayed processing of all measurements and these algorithms tend to be computationally rather demanding. The recursive type are generally Kalman filter based and are not computationally restrictive. Thus, for airborne applications, it is desirable to use recursive type angle-only TMA algorithms.

This report presents the work done in the first stage of the study on passive ranging in jamming conditions. In particular, it presents a comparison of six recursive style angle-only TMA algorithms which are applicable to the tracking problem in a jamming situation. The algorithms considered are,

1. Cartesian coordinate EKF,
2. Pseudo-Linear estimator,
3. Modified gain EKF,
4. Modified Polar coordinate EKF,
5. Range-Parameterised Cartesian coordinate EKF, and
6. Range-Parameterised Modified Polar coordinate EKF.

All algorithms are based on filters which are derivatives of either the standard or the extended Kalman filter. The first four algorithms consist of single filters, and the last two are based on a weighted sum of multiple filter outputs. Except for algorithms (4) and (6), they are formulated in Cartesian coordinates. Algorithms (4) and (6) are derived in a different coordinate system called Modified Polar coordinates.

Throughout the report, we make the following assumptions. First, we are tracking a single non-maneuvering target[1] which uses ECM, with the assumption that the angle measurements are reliable. Second, we assume that the jamming has already started and we have detected its occurrence, i.e., we ignore for the time being the transition from a

[1]At a later stage this will be extended to the case of a maneuvering target.

non-jammed to a jammed situation. Finally, for simplicity we assume 2-D measurements, although in airborne applications the measurements are in 3-D[2].

The organisation of the report is as follows. Section 2 describes the angle-only TMA problem in detail, and sets the mathematical framework for its solution. Sections 3-7 present the six aformentioned angle-only TMA algorithms. In each of the sections 3-7, a brief summary of the algorithm development and some known properties pertaining to the algorithm are given. Simulation results for the algorithms are described in Section 8, followed by some concluding remarks in Section 9.

2 The Angle-only TMA Problem

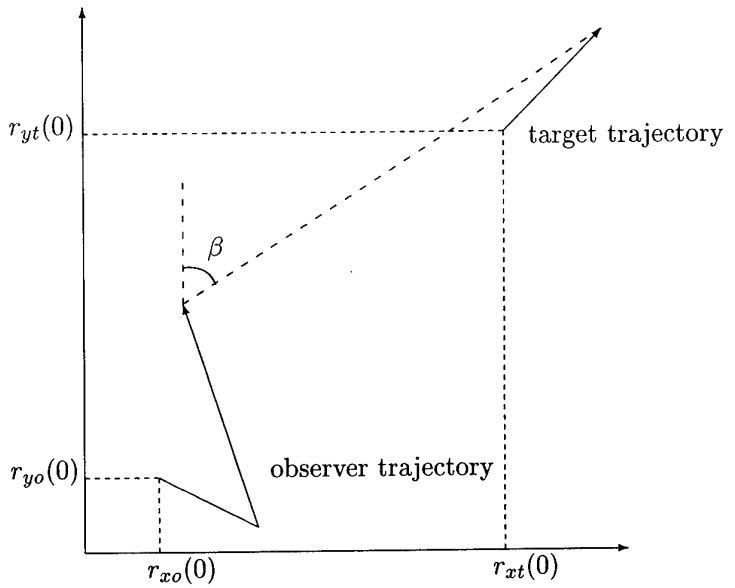

Figure 1: Typical two-dimensional target-observer geometry

Conceptually, the basic problem in angle-only TMA is to estimate the trajectory of a target (i.e., position and velocity) from noise corrupted sensor angle data. For the case of a single-sensor problem, these angle data are obtained from a single moving observer (ownship). To define the problem mathematically, consider the two-dimensional angle-only TMA problem, where a typical target-observer encounter is depicted in Fig 1. The target, located at coordinates (r_{xt}, r_{yt}) moves with a constant velocity vector $[v_{xt}, v_{yt}]$ and is defined to have the state vector

$$X_t = [r_{xt}, r_{yt}, v_{xt}, v_{yt}]',$$

where the prime denotes transpose. The observer state is similarly defined as

$$X_o = [r_{xo}, r_{yo}, v_{xo}, v_{yo}]',$$

[2]The extension from 2-D to 3-D has conceptually been solved in the literature [8].

where the velocity vector need not be constant. By introducing the relative state vector, defined by

$$X = X_t - X_o = [r_x, r_y, v_x, v_y]'$$

the discrete time state equation for this problem can be written as

$$X(k+1) = \Phi(k+1,k)X(k) - U(k,k+1), \tag{1}$$

where

$$\Phi(k+1,k) = \begin{bmatrix} 1 & 0 & T & 0 \\ 0 & 1 & 0 & T \\ 0 & 0 & 1 & 0 \\ 0 & 0 & 0 & 1 \end{bmatrix} \tag{2}$$

is the transition matrix, T is the sampling time, and

$$U(k,k+1) = \begin{bmatrix} u_1(k,k+1) \\ u_2(k,k+1) \\ u_3(k,k+1) \\ u_4(k,k+1) \end{bmatrix} = \begin{bmatrix} r_{xo}(k+1) - r_{xo}(k) - Tv_{xo} \\ r_{yo}(k+1) - r_{yo}(k) - Tv_{yo} \\ v_{xo}(k+1) - v_{xo}(k) \\ v_{yo}(k+1) - v_{yo}(k) \end{bmatrix} \tag{3}$$

is a vector of deterministic inputs which account for the effects of observer accelerations. Observe that the state dynamics equation (1) does not contain a process noise term as we are assuming a constant velocity target model. Also, note that $U(\cdot,\cdot)$ is deterministic since we implicitly assume that we have knowledge of the observer state X_o at every instant in time[3].

The available measurement at time k is the angle from the observer's platform to the target, referenced (clockwise positive) to the y-axis (i.e., angle between y-axis and line-of-sight, see Fig 1), and is given by

$$\beta(k) = \tilde{\beta}(k) + \nu(k), \tag{4}$$

where $\nu(k)$ is a zero mean independent Gaussian noise with variance σ_β^2 and $\tilde{\beta}(k)$ is the noise-free angle

$$\tilde{\beta}(k) = \tan^{-1}\left[\frac{r_x(k)}{r_y(k)}\right] \tag{5}$$

Given a sequence of measurements $\beta(k)$, $k = 1, 2, \ldots$, defined by (4) and (5), and target motion model described in (1), (2) and (3), the angle-only TMA problem is to obtain estimates of the state vector $X(k)$ (and hence $X_t(k)$).

3 The Cartesian Coordinate EKF

3.1 Introduction

The angle-only TMA problem in Cartesian coordinates is non-linear since the measurement equation (5) is non-linear. Therefore, linear filtering algorithms such as the

[3]The knowledge of the observer coordinates and velocities is provided by an on-board INS (inertial navigation system), usually supervised by a GPS system.

standard Kalman filter are not applicable and one must resort to non-linear methods such as extended Kalman filters [4]. One of the first algorithms employed to solve the angle-only TMA problem was an extended Kalman filter in Cartesian coordinates [1, 2]. This filter, known as the Cartesian coordinate Extended Kalman Filter (CEKF) uses state dynamics and measurement models that are formulated in Cartesian coordinates.

3.2 Development of the Algorithm

In order to apply the principles of Kalman Filter theory to the angle-only TMA problem, the measurement equation (4) is re-written to show clearly the relationship between the measurement and state:

$$\beta(k) = h\left[X(k)\right] + \nu(k), \tag{6}$$

where

$$h\left[X(k)\right] = \tan^{-1}\left[\frac{r_x(k)}{r_y(k)}\right]. \tag{7}$$

Now, although the target motion model given by (1), (2) and (3) is linear, the measurement model of (6) and (7) is non-linear. Thus, we employ an Extended Kalman Filter (EKF) which is derived by linearising (7) and using an equivalent measurement matrix (evaluated at the predicted state) in the ordinary Kalman Filter equations.

The Cartesian EKF algorithm for the angle-only TMA problem is presented below. First, we define the terms

$\hat{X}(0|0)$ - Initial estimate of the state
$P(0|0)$ - Initial estimate of the state error covariance
$\hat{X}(k|k)$ - State estimate at k, based on k measurements
$P(k|k)$ - Estimate of state error covariance at k, based on k measurements

Now, suppose we have $\hat{X}(k|k)$ and its associated error covariance matrix $P(k|k)$. Then, the updated state $\hat{X}(k+1|k+1)$, and its covariance $P(k+1|k+1)$ based on $k+1$ measurements can be computed as follows [2].

Using $\hat{X}(k|k)$ and $P(k|k)$, the predicted state $\hat{X}(k+1|k)$ at $k+1$ and its error covariance $P(k+1|k)$ based on k measurements are computed as

$$\hat{X}(k+1|k+1) = \Phi(k+1,k)\hat{X}(k|k) - U(k,k+1) \tag{8}$$

$$P(k+1|k) = \Phi(k+1,k)P(k|k)\Phi(k+1,k)' \tag{9}$$

The Kalman gain matrix, which is used in computing the updated state, can now be evaluated as

$$G(k+1) = P(k+1|k)H(k+1)'\left[H(k+1)P(k+1|k)H(k+1)' + \sigma_\beta^2(k+1)\right]^{-1} \tag{10}$$

[4] Other filtering schemes, designed for non-linear/non-Gaussian models, such as particle or bootstrap filtering [12, 16] have not been considered here as they are computationally very expensive for real-time applications.

where $H(k+1)$ is the equivalent measurement matrix (evaluated at the predicted state), given by

$$\begin{aligned} H(k+1) &= \left.\frac{\partial h[X(k+1)]}{\partial X}\right|_{X=\hat{X}(k+1|k)} \\ &= \left[\frac{\hat{r}_y(k+1|k)}{\hat{r}_x(k+1|k)^2+\hat{r}_y(k+1|k)^2}, \frac{-\hat{r}_x(k+1|k)}{\hat{r}_x(k+1|k)^2+\hat{r}_y(k+1|k)^2}, 0, 0\right] \end{aligned} \quad (11)$$

The updated state and its covariance matrix are given by

$$\hat{X}(k+1|k+1) = \hat{X}(k+1|k) + G(k+1)\left[\beta(k+1) - \hat{\beta}(k+1|k)\right] \quad (12)$$

$$P(k+1|k+1) = [I - G(k+1)H(k+1)]\,P(k+1|k), \quad (13)$$

where I is the 4×4 Identity matrix and $\hat{\beta}(k+1|k) = h[\hat{X}(k+1|k)]$.

Equations (8)-(13) constitute the EKF in the Cartesian coordinates. Some comments on initialisation of state estimate and its covariance are in order here. In general, for reliable performance of the EKF, the initialisation is critical, and thus some *a priori* knowledge of the range and allowable speeds for the target is helpful. Suppose we have some *a priori* knowledge of the mean of the initial range and its variance, given by $\bar{r}$ and σ_r^2, respectively. Also, suppose the target moves with a speed less than s_{max}. If a certain distribution of the speeds is assumed, one can ascertain the variance σ_v^2 corresponding to the velocity of the target. With the above assumptions, the state and its covariance can be initialised as follows:

$$\hat{X}(0|0) = [\bar{r}\sin\beta(0), \bar{r}\cos\beta(0), 0, 0]', \quad (14)$$

$$P(0|0) = \text{diag}\left[\sigma_r^2, \sigma_r^2, \sigma_v^2, \sigma_v^2\right], \quad (15)$$

where $\beta(0)$ is the initial angle measurement.

3.3 Properties and Performance of the Algorithm

The properties and performance of the Cartesian coordinate EKF is well documented [1, 2]. In general, this algorithm is not always guaranteed to work, and its performance depends on measurement noise levels and on proper initialisation of the state and associated covariance matrix. Furthermore, in order to be able to track the target with angle-only measurements, it has been found [1, 2] that the observer must maneuver[5]. The commonly observed problem with the Cartesian EKF is the premature collapse of the error covariance matrix even prior to an observer maneuver. What this means is that the error bounds of the estimate, even though they should remain high prior to an observer maneuver, rapidly deteriorate to a small value. Tight error bounds around the current estimate give little or no room at all to correct the estimate and filter divergence results. The cause for this error covariance matrix collapse is the dependence of the computation of error covariance matrices on state estimates. In particular, if the state estimates are in error, this would result in an incorrect estimation of the covariance matrices.

[5]This result is applicable to all angle-only TMA algorithms

4 The Pseudo-Linear Estimator

4.1 Introduction

It was mentioned earlier that the Cartesian EKF suffers from filter divergence caused by premature covariance matrix collapse. This is the result of the dependence of the covariance computation on state estimates which could be in error. To eliminate this problem, a new algorithm, called the Pseudo-Linear Estimator (PLE) was proposed [2, 3] which essentially decouples the covariance matrix computations from the estimated state vector. The decoupling technique involves replacing measured angles with Pseudo-Linear measurement residuals [2, 3] as will be seen shortly. An attractive feature of this approach is that it permits a solution to the angle-only TMA problem via linear estimation theory.

4.2 Development of the Algorithm

To derive the Pseudo linear estimator, observe that the non-linear equations (6) and (7) can be algebraically manipulated to yield a new measurement equation [3]

$$0 = \tilde{H}(k)X(k) + \epsilon(k), \tag{16}$$

where

$$\begin{aligned} \tilde{H} &= [\cos\beta(k), -\sin\beta(k), 0, 0]\,, \\ \epsilon(k) &= r(k)\sin\nu(k), \\ r(k) &= \sqrt{r_x(k)^2 + r_y(k)^2}, \end{aligned} \tag{17}$$

and $\beta(k)$ is the measured angle at time k. Note that though (16) appears linear, the nonlinearity in (6) and (7) has been embedded in the new measurement noise term $\epsilon(k)$ which is a function of the state.

In order to use Kalman filter theory, we assume $\epsilon(k)$ to be a white Gaussian process and independent of the initial state estimate. This does not really hold since $\epsilon(k)$ is neither normally distributed nor white. However, for the purpose of applying Kalman filter equations, we continue to use the white Gaussian assumption for $\epsilon(k)$ which has first and second moments given by [3]

$$\begin{aligned} E\left[\epsilon(k)\right] &= 0 \\ E\left[\epsilon^2(k)\right] &= \frac{r^2(k)}{2}\left(1 - e^{-2\sigma_\beta^2(k)}\right) \\ &\approx r^2(k)\sigma_\beta^2(k), \quad \sigma_\beta^2(k) \ll 1 \end{aligned}$$

Now, the Kalman filter corresponding to the new measurement equation (16) may be derived from (8)-(13) by replacing certain terms with others. In particular, if

$$\hat{r}(k+1|k) = \sqrt{\hat{r}_x^2(k) + \hat{r}_y^2(k)},$$

the Pseudo-Linear estimator is obtained by replacing $H(k)$ with $\tilde{H}(k)$, $\sigma_\beta(k+1)$ with $\hat{r}(k+1|k)\sigma_\beta(k+1)$, and $\{\beta(k+1) - h[\hat{X}(k+1|k)]\}$ with $-\tilde{H}(k+1)\hat{X}(k+1|k)$. However, it has been argued [3] that if the initial covariance matrix and the effective measurement noise variance are appropriately normalised, replacing $\sigma_\beta(k+1)$ with $\hat{r}(k+1|k)\sigma_\beta(k+1)$ is unnecessary. Furthermore, the initialisation of state and its covariance matrix were set to be the null vector and identity matrix, respectively. Thus, the Pseudo-Linear estimator algorithm takes the form [3]

$$\begin{aligned}
\hat{X}(0|0) &= \mathbf{0}, \\
P(0|0) &= I, \\
\hat{X}(k+1|k) &= \Phi(k+1,k)\hat{X}(k|k) - U(k,k+1) \\
P(k+1|k) &= \Phi(k+1,k)P(k|k)\Phi(k+1,k)' \\
\tilde{H}(k+1) &= [\cos\beta(k+1), -\sin\beta(k+1), 0, 0] \\
G(k+1) &= P(k+1|k)\tilde{H}(k+1)'\left[\tilde{H}(k+1)P(k+1|k)\tilde{H}(k+1)' + \sigma_\beta^2(k+1)\right]^{-1} \\
\hat{X}(k+1|k+1) &= \hat{X}(k+1|k) - G(k+1)\tilde{H}(k+1)\hat{X}(k+1|k) \\
P(k+1|k+1) &= \left[I - G(k+1)\tilde{H}(k+1)\right]P(k+1|k)
\end{aligned} \tag{18}$$

4.3 Properties and Performance of the Algorithm

The performance analysis of this Pseudo-Linear filter is presented in [2, 3]. It is shown that estimates of the target's velocity are asymptotically unbiased, but the estimated range exhibits steady-state bias. The reason for this bias is attributed to the fact that the measurement matrix $\tilde{H}$ contains elements that are functions of noisy angles and are correlated with the noise terms. In particular, the gain matrix is correlated with the residual (difference between actual and predicted measurements) which causes the PLE to exhibit bias. However, the performance analysis also showed that the filter performed well under low measurement noise levels or high angle rates, which generally characterises a close range target-observer scenario.

5 The Modified Gain EKF

5.1 Introduction

Recall that the Cartesian EKF exhibited filter instability due to the dependence of the covariance computations on the state estimates. To eliminate this problem, the Pseudo-Linear estimator was proposed which had a linear measurement equation with non-linearities embedded in a new noise term. Although the covariance computations are independent of the state estimates, the gain matrix is correlated with the residual and this resulted in biased estimates. The Modified Gain Extended Kalman Filter (MGEKF) [10] attempts to alleviate both problems of the previous filters. In particular, it is designed to produce estimates that are both stable as well as asymptotically unbiased.

5.2 Development of the Algorithm

The MGEKF algorithm is derived by observing that one can write [11]

$$\tilde{\beta}(k+1) - \hat{\beta}(k+1|k) = \bar{H}_1(k+1)\left[X(k+1) - \hat{X}(k+1|k)\right] \tag{19}$$

where $\tilde{\beta}(k+1)$ is the noise-free angle at $k+1$, $\hat{\beta}(k+1|k)$ is the predicted angle at $k+1$ based on k measurements, and

$$\bar{H}_1(k+1) = \left[\frac{\cos\tilde{\beta}(k+1), -\sin\tilde{\beta}(k+1)}{\hat{r}_x(k+1|k)\sin\tilde{\beta}(k+1) + \hat{r}_y(k+1|k)\cos\tilde{\beta}(k+1)}, 0, 0\right]. \tag{20}$$

Now, using (19) in (12) and substituting the measured angle $\beta(k+1)$ for $\tilde{\beta}(k+1)$, (12) can be re-written as

$$\hat{X}(k+1|k+1) = \hat{X}(k+1|k) + G(k+1)\bar{H}(k+1)\left[X(k+1) - \hat{X}(k+1|k)\right] \tag{21}$$

where

$$\bar{H}(k+1) = \left[\frac{\cos\beta(k+1), -\sin\beta(k+1)}{\hat{r}_x(k+1|k)\sin\beta(k+1) + \hat{r}_y(k+1|k)\cos\beta(k+1)}, 0, 0\right]. \tag{22}$$

Observe that the filter update equation of (21) looks linear with measurement matrix $\bar{H}(k+1)$. Thus, we could replace the matrix $H(k+1)$ with $\bar{H}(k+1)$ in the Cartesian EKF equations (8)-(13). However, in the gain computation equation (10), if $\bar{H}(k+1)$ is used instead of $H(k+1)$, biased estimates are expected since the gain and the residual will then be directly correlated in a manner similar to the Pseudo-Linear filter. Thus, a gain equation similar to (10) which ensures that the gain is a function of the past measurements only is desirable. Now, notice that

$$\begin{aligned} H(k+1) &= \left[\frac{\hat{r}_y(k+1|k), -\hat{r}_x(k+1|k)}{\hat{r}_x(k+1|k)^2 + \hat{r}_y(k+1|k)^2}, 0, 0\right] \\ &= \left[\frac{\cos\hat{\beta}(k+1|k), -\sin\hat{\beta}(k+1|k)}{\hat{r}_x(k+1|k)\sin\hat{\beta}(k+1|k) + \hat{r}_y(k+1|k)\cos\hat{\beta}(k+1|k)}, 0, 0\right]. \end{aligned} \tag{23}$$

which is essentially the $\bar{H}(k+1)$ matrix with the measured angle $\beta(k+1)$ replaced by the predicted angle $\hat{\beta}(k+1|k)$. Thus, in replacing $H(k+1)$ with $\bar{H}(k+1)$ in the gain equation (10), we substitute the predicted angle $\hat{\beta}(k+1|k)$ for the measured angle. Note from (23) that this is equivalent to leaving (10) unaltered! Thus, the only modification required in the equation set (8)-(13) is the replacing of $H(k+1)$ with $\bar{H}(k+1)$ in the covariance update equation (13). A summary of the MGEKF algorithm is as follows:

$$\begin{aligned} \hat{X}(k+1|k) &= \Phi(k+1,k)\hat{X}(k|k) - U(k,k+1) \\ P(k+1|k) &= \Phi(k+1,k)P(k|k)\Phi(k+1,k)' \\ H(k+1) &= \left[\frac{\cos\hat{\beta}(k+1|k), -\sin\hat{\beta}(k+1|k)}{\hat{r}_x(k+1|k)\sin\hat{\beta}(k+1|k) + \hat{r}_y(k+1|k)\cos\hat{\beta}(k+1|k)}, 0, 0\right] \\ G(k+1) &= P(k+1|k)H(k+1)'\left[H(k+1)P(k+1|k)H(k+1)' + \sigma_\beta^2(k+1)\right]^{-1} \end{aligned}$$

$$\begin{aligned}
\hat{X}(k+1|k+1) &= \hat{X}(k+1|k) + G(k+1)\left[\beta(k+1) - \hat{\beta}(k+1|k)\right] \\
\bar{H}(k+1) &= \left[\frac{\cos\beta(k+1), -\sin\beta(k+1)}{\hat{r}_x(k+1|k)\sin\beta(k+1) + \hat{r}_y(k+1|k)\cos\beta(k+1)}, 0, 0\right]. \\
P(k+1|k+1) &= \left[I - G(k+1)\bar{H}(k+1)\right] P(k+1|k) \qquad (24)
\end{aligned}$$

The MGEKF algorithm can be initialised in a similar manner to that of the Cartesian EKF.

5.3 Properties and Performance of the Algorithm

The performance of this algorithm is documented in [10, 11]. It was found that the MGEKF algorithm results in stable and asymptotically unbiased estimates. The estimates are stable since the computation of the covariance update uses the $\bar{H}(k+1)$ matrix in which measured angle is used, instead of $H(k+1)$ in which the estimated angle is employed. Furthermore, the asymptotic unbiasedness is due to the fact that the gain matrix is uncorrelated with the residual. Thus, the MGEKF has retained the best properties of the ordinary Cartesian EKF and the Pseudo-Linear estimator.

6 The Modified Polar Coordinate EKF

6.1 Introduction

It has been shown that the estimation algorithms for the angle-only TMA problem formulated in Cartesian coordinates have resulted in unstable and biased estimates. Specifically, the Cartesian coordinate EKF exhibits filter divergence while the Pseudo-Linear estimator shows biased characteristics. To overcome these difficulties, a new extended Kalman filter was proposed [4], which was formulated in a different coordinate system called the Modified Polar (MP) coordinates. This coordinate system was shown to be well suited for angle-only target motion analysis because it automatically decouples observable and unobservable components of the estimated state vector. Such decoupling prevents covariance matrix ill-conditioning which is the primary cause of filter instability.

The MP state vector is comprised of the following four components: angle, angle rate, range rate divided by range, and the reciprocal of range. In theory, the first three can be determined from single-sensor angle data without an ownship maneuver; the fourth component, however, remains unobservable until a maneuver occurs.

6.2 Development of the Algorithm

To derive the Modified Polar coordinate Extended Kalman Filter (MPEKF), consider the state dynamics and measurement equations for the angle-only TMA problem in Cartesian coordinates which are repeated here for convenience,

$$X(k+1) = \Phi(k+1,k)X(k) - U(k,k+1) \qquad (25)$$

$$\beta(k) = h_x\left[X(k)\right] + \nu(k) \tag{26}$$

where $\Phi(\cdot,\cdot)$ and $U(\cdot,\cdot)$ are defined in (2) and (3), respectively, and

$$h_x\left[X(k)\right] = \tan^{-1}\left[\frac{r_x(k)}{r_y(k)}\right] \tag{27}$$

$$\begin{aligned} X(k) &= [x_1(k), x_2(k), x_3(k), x_4(k)]' \\ &= [r_x(k), r_y(k), v_x(k), v_y(k)]'. \end{aligned}$$

Note that the subscript x in $h_x[\cdot]$ denotes the $h[\cdot]$ function in Cartesian coordinates.

The first step in deriving the EKF in MP coordinates is to derive an equivalent set of state dynamics and measurement equation as in (25), (26) and (27) in these coordinates. This turns out to be difficult if conventional modeling techniques are employed as the transformed equations of motion are highly nonlinear in these coordinates. Fortunately, the difficulties with the conventional approach can be avoided by recognising that we can derive the required equations by algebraic manipulations. To see this, let $Y(k)$ denote the MP state vector:

$$\begin{aligned} Y(k) &= [y_1(k), y_2(k), y_3(k), y_4(k)]' \\ &= \left[\dot{\beta}(k), \frac{\dot{r}(k)}{r(k)}, \beta(k), \frac{1}{r(k)}\right]' \end{aligned} \tag{28}$$

Now, it can be established, as will be seen below, that $X(k)$ and $Y(k)$ are related at all times by the non-linear one-to-one transformations

$$X(k) = f_x\left[Y(k)\right] \tag{29}$$

$$Y(k) = f_y\left[X(k)\right] \tag{30}$$

To derive these transformations, we note the following relationships between Cartesian and polar coordinates:

$$\begin{aligned} r_x &= r\sin\beta \\ r_y &= r\cos\beta \\ v_x &= \dot{r}_x = \dot{r}\sin\beta + r\dot{\beta}\cos\beta \\ v_y &= \dot{r}_y = \dot{r}\cos\beta - r\dot{\beta}\sin\beta \end{aligned} \tag{31}$$

and

$$\begin{aligned} \beta &= \tan^{-1}\left(\frac{r_x}{r_y}\right) \\ \dot{\beta} &= \frac{(r_y v_x - r_x v_y)}{(r_x^2 + r_y^2)} \\ r &= \sqrt{r_x^2 + r_y^2} \\ \dot{r} &= \frac{(r_x v_x + r_y v_y)}{\sqrt{r_x^2 + r_y^2}} \end{aligned} \tag{32}$$

From (31) and (32), we can obtain the necessary functions $f_x[\cdot]$ and $f_y[\cdot]$, and the result is [4, 9]

$$\begin{aligned} X(k) &= f_x\left[Y(k)\right] \\ &= \frac{1}{y_4(k)} \begin{bmatrix} \sin y_3(k) \\ \cos y_3(k) \\ y_2(k)\sin y_3(k) + y_1(k)\cos y_3(k) \\ y_2(k)\cos y_3(k) - y_1(k)\sin y_3(k) \end{bmatrix} \end{aligned} \tag{33}$$

and

$$\begin{aligned} Y(k) &= f_y\left[X(k)\right] \\ &= \begin{bmatrix} \left[x_3(k)x_2(k) - x_4(k)x_1(k)\right] / \left[x_1^2(k) + x_2^2(k)\right] \\ \left[x_3(k)x_1(k) + x_4(k)x_2(k)\right] / \left[x_1^2(k) + x_2^2(k)\right] \\ \tan^{-1}\left[x_1(k)/x_2(k)\right] \\ 1 \Big/ \sqrt{x_1^2(k) + x_2^2(k)} \end{bmatrix} \end{aligned} \tag{34}$$

Now, substituting (33) for $X(k)$ in (25), we get

$$X(k+1) = \Phi(k+1,k) f_x\left[Y(k)\right] - U(k,k+1) \tag{35}$$

By using the transformation (34) for $Y(k+1)$, it follows that

$$\begin{aligned} Y(k+1) &= f_y\left[X(k+1)\right] \\ &= f_y\left[\Phi(k+1,k) f_x\left[Y(k)\right] - U(k,k+1)\right] \\ &= f\left[Y(k); k, k+1\right] \end{aligned} \tag{36}$$

It can be shown using (33), (34) and (36) that

$$\begin{aligned} f\left[Y(k); k, k+1\right] &= \left[f_1, f_2, f_3, f_4\right]' \\ &= \begin{bmatrix} (\alpha_2\alpha_3 - \alpha_1\alpha_4)/(\alpha_1^2 + \alpha_2^2) \\ (\alpha_1\alpha_3 + \alpha_2\alpha_4)/(\alpha_1^2 + \alpha_2^2) \\ y_3(k) + \tan^{-1}(\alpha_1/\alpha_2) \\ y_4(k)/(\alpha_1^2 + \alpha_2^2)^{1/2} \end{bmatrix} \end{aligned} \tag{37}$$

where α_i, $i = 1, \ldots, 4$ are functions of $Y(k)$ and $U(k, k+1)$, given by

$$\begin{aligned} \alpha_1 &= Ty_1(k) - y_4(k)\left[u_1(k,k+1)\cos\beta(k) - u_2(k,k+1)\sin\beta(k)\right] \\ \alpha_2 &= 1 + Ty_2(k) - y_4(k)\left[u_1(k,k+1)\sin\beta(k) + u_2(k,k+1)\cos\beta(k)\right] \\ \alpha_3 &= y_1(k) - y_4(k)\left[u_3(k,k+1)\cos\beta(k) - u_4(k,k+1)\sin\beta(k)\right] \\ \alpha_4 &= y_2(k) - y_4(k)\left[u_3(k,k+1)\sin\beta(k) - u_4(k,k+1)\cos\beta(k)\right] \end{aligned} \tag{38}$$

Similarly, the measurement equation can be expressed in Modified Polar coordinates by substituting (33) in (26), i.e.,

$$\begin{aligned} \beta(k) &= h_y\left[Y(k)\right] + \nu(k) \\ &= \left[0,0,1,0\right] Y(k) + \nu(k) \end{aligned} \tag{39}$$

Equations (36) and (39) are exact analogs of (25) and (26). We note that the measurement equation (39) is linear while the state dynamics equation (36) is non-linear. Straightforward application of the EKF to (36) and (39) will now yield the Modified Polar coordinate EKF described below.

$$\begin{aligned}
\hat{Y}(0|0) &= \text{Initial estimate of MP state vector} \\
P(0|0) &= \text{Initial estimate of MP state vector error covariance matrix} \\
\hat{Y}(k+1|k) &= f\left[\hat{Y}(k|k); k, k+1\right] \\
F(k+1,k) &= \left.\frac{\partial f\left[Y(k); k, k+1\right]}{\partial Y}\right|_{Y=\hat{Y}(k|k)} \\
P(k+1|k) &= F(k+1,k)P(k|k)F(k+1,k) \\
H_y &= [0,0,1,0] \\
G(k+1) &= P(k+1)H_y'\left[H_y P(k+1|k)H_y' + \sigma_\beta^2(k+1)\right]^{-1} \\
\hat{Y}(k+1|k+1) &= \hat{Y}(k+1|k) + G(k+1)\left[\beta(k+1) - H_y\hat{Y}(k+1|k)\right] \\
P(k+1|k+1) &= \left[I - G(k+1)H_y\right]P(k+1|k)
\end{aligned} \tag{40}$$

Note that the computation of the linearised transition matrix $F(k+1,k)$ is described in the appendix.

Comment on the filter initialisation problem is in order here. To obtain reasonably good initial estimates, one could use some batch processing techniques and then apply the MPEKF. Otherwise, an initialisation approach suggested in [13] can be employed. In [13] it is assumed that we have knowledge of the mean of the initial range, $\bar{r}$, and its variance σ_r^2. Also, suppose the velocity error standard deviation, σ_v, is known. Then, the MPEKF can be initialised according to [13] as

$$\hat{Y}(0|0) = [0, 0, \beta(0), 1/\bar{r}]',$$

where $\beta(0)$ is the initial angle measurement. The corresponding state error covariance matrix is initialised to be [13]

$$P(0|0) = \text{diag}\,[\sigma_{\dot{\beta}}^2, \sigma_{\dot{R}/R}^2, \sigma_\beta^2, \sigma_{1/R}^2]'$$

where

$$\begin{aligned}
\sigma_{\dot{\beta}} &= \sigma_v/\bar{r} \\
\sigma_{\dot{R}/R} &= \sigma_v/\bar{r} \\
\sigma_\beta &= \text{measurement standard deviation} \\
\sigma_{1/R} &= \sigma_r/\bar{r}^2
\end{aligned}$$

6.3 Properties and Performance of the Algorithm

The performance of the Modified Polar coordinate EKF has been documented in [4, 9]. The analysis showed that MPEKF outperforms the Cartesian EKF and Pseudo-Linear estimator in both short and long range scenarios. Furthermore, it was found that MPEKF is both stable and asymptotically unbiased.

7 Range Parameterised EKF Trackers

7.1 Introduction

This section presents a new angle-only TMA approach which consists of a set of weighted EKFs, each with a different initial range estimate. The tracker, referred to as Range-Parameterised (RP) tracker, is particularly useful when there is very little *a priori* knowledge of the initial target range. Two range-parameterised trackers will be considered in this report: a) Range-Parameterised Cartesian coordinate EKF (RPCEKF), and b) Range-Parameterised Modified Polar coordinate EKF (RPMPEKF). The principles involved in these two trackers are essentially the same, and thus the rest of this section will introduce the concepts applicable to both algorithms.

7.2 General Principles

The tracking approach of the RP EKF trackers is to track the state of the target with a number of independent EKF trackers, each with a different initial range estimate. To do so, the range interval of interest is divided into a number of subintervals, and each subinterval is tracked with an independent EKF.

Suppose the range interval of interest is (R_{min}, R_{max}), and we wish to track using N_F EKF filters. For a particular EKF, we note that the tracking performance is highly dependent on the *Coefficient of Variation* of the range estimate [13], C_R, given by σ_R/R, where R and σ_R are the range estimate and its standard deviation, respectively. In order to maintain a comparable performance for all N_F filters, it is desirable to subdivide the interval (R_{min}, R_{max}) such that C_R is the same for each subinterval. Note that C_R for each subinterval may be computed approximately as σ_{R_i}/R_i, where R_i is the mean of subinterval i and σ_{R_i} is the range standard deviation for that subinterval. Assuming the range errors to be uniformly distributed in each subinterval, the desirable subdivision can be obtained if the subinterval boundaries are chosen as a geometrical progression. If ρ is the common ratio, we have the relation

$$R_{max} = R_{min}\rho^{N_F},$$

which gives ρ as

$$\rho = \left(\frac{R_{max}}{R_{min}}\right)^{1/N_F}.$$

For the above division of range, it is easily established [15] that the coefficient of variation is given by

$$C_R = \frac{\sigma_{R_i}}{R_i} = \frac{2(\rho-1)}{\sqrt{12}(\rho+1)}. \tag{41}$$

To determine how the state estimate of each filter is combined, we need to compute the weights associated with each EKF. At time step 1, let the probability that the true track originated from the i-th subinterval be denoted by $\text{Prob}(i,1)$. These probabilities,

which form the initial weights for the RP tracker, can be obtained from a uniform distribution when no prior information about the true range is available. The corresponding probabilities at time k can be computed recursively according to Bayes' rule,

$$\text{Prob}(i,k) = \frac{\text{Prob}(\beta(k)|i)\,\text{Prob}(i,k-1)}{\sum_{j=1}^{N_F}\text{Prob}(\beta(k)|j)\,\text{Prob}(j,k-1)} \tag{42}$$

where $\text{Prob}(\beta(k)|i)$ is the likelihood of measurement $\beta(k)$, given that the target originated in subinterval i. Assuming Gaussian statistics, this can be computed as [13]

$$\text{Prob}(\beta(k)|i) = \frac{1}{\sqrt{2\pi\sigma^2}}\exp\left[-\frac{1}{2}\left(\frac{\beta(k)-\hat{\beta}(k,i|k-1)}{\sigma}\right)^2\right] \tag{43}$$

where $\hat{\beta}(k,i|k-1)$ is the predicted angle at k for filter i, and σ^2 is the innovation variance given by

$$\sigma^2 = H(k)P(k|k-1)H(k)' + \sigma_\beta^2(k), \tag{44}$$

where $H(\cdot)$ is the linearised measurement matrix, and $\sigma_\beta^2(k)$ is the variance of the measured angle.

Now, suppose the updated state estimate of filter i (corresponding to subinterval i) is denoted by $\hat{X}(k,i|k)$. Then, the updated state estimate of the RP tracker can be computed as a weighted sum of the individual estimates [15],

$$\hat{X}(k|k) = \sum_{i=1}^{N_F}\text{Prob}(i,k)\hat{X}(k,i|k). \tag{45}$$

Similarly, if $P(k,i|k)$ denotes the covariance matrix of the i-th filter at k, the corresponding covariance for the RP tracker may be computed as [15]

$$P(k|k) = \sum_{i=1}^{N_F}\text{Prob}(i,k)\left[P(k,i|k) + (\hat{X}(k,i|k)-\hat{X}(k|k))(\hat{X}(k,i|k)-\hat{X}(k|k))'\right]. \tag{46}$$

The improved tracking performance of the RP tracker is achieved by tracking N_F independent EKF trackers, each with a much smaller coefficient of variation than would be required by a single EKF. This improvement is achieved at the expense of an N_F-fold increase in computations if all the range subintervals are processed throughout. However, it has been found [13] that in a majority of target-observer scenarios, the weighting of some of the subintervals rapidly reduces to zero. In such cases, the corresponding filters can be removed from the tracking process without loss of accuracy, thereby reducing the processing requirement. Thus, a weighting threshold can be set and any filter corresponding to a subinterval with a weight less than the threshold may be removed from the tracking process.

The tracker initialisation for RP-Cartesian and RP-Modified Polar EKFs are carried out according to the principles discussed in sections 3.2 and 6.2, respectively. The only changes required are, for filter i the mean of the range is replaced by R_i (mean of subinterval i), and the range standard deviation is replaced by σ_{R_i} (range standard deviation for subinterval i), assuming range errors to be uniformly distributed in that subinterval.

7.3 Properties and Performance of the Algorithms

The properties and performance of the RPCEKF and RPMPEKF are well documented in [15] and [13], respectively. It is found that the RP trackers show better tracking performance than the CEKF or MPEKF trackers in a typical tracking scenario. In addition, the RP tracker is found to be stable even under adverse tracking conditions such as when the angle rate is very high or near zero. The improved tracking performance is achieved due to the fact that the RP tracker divides the large prior range uncertainty region into a number of smaller subintervals, each with a lower coefficient of variation than the single-filter trackers. Since a number of EKFs are processed in parallel, this improvement comes at the expense of increased processing. However, it is found that in most cases, the weighting of some filters reduces rapidly to zero. When this occurs, those filters can be removed from the tracking process without loss of accuracy, resulting in a tracker that is not so computationally intensive.

8 Simulation Results

To illustrate the angle-only tracking performance for the algorithms described in this report, the algorithms were implemented in Matlab and simulations were set up for two scenarios. Scenario 1 corresponds to an initial target range of 35 km while the same parameter for scenario 2 is 70 km. The target maintains a constant speed and bearing of 200 km/h and 45°, respectively. Ownship also maintains a constant speed of 600 km/h, but periodically executes 90° course changes as follows:

$$\begin{aligned} &\text{from } 90^\circ \text{ to } 0^\circ \text{ at } t = (10 + 40k)T \text{ sec}, \quad k = [0, 1, 2] \\ &\text{from } 0^\circ \text{ to } 90^\circ \text{ at } t = (30 + 40k)T \text{ sec}, \quad k = [0, 1] \end{aligned}$$

where the sampling time $T = 3$ sec. The target-observer geometry for the simulations is depicted in Fig 2. Angle measurements were sampled for a total period of 300 sec (5 minutes). Note that the above course changes correspond to a total of five maneuvers (i.e., maneuvers are carried out at $(10, 30, 50, 70, 90) \times T$ sec) during the observation period. For all simulations, the angle measurement noise was set at $\sigma_\beta = 2.5^\circ$. The initialisation of the state vector and its covariance matrix were carried out as follows. The PLE algorithm was initialised according to section 4 where the initialisation was found to be independent of the parameters of the scenario. For the other algorithms, the initial range estimates for scenarios 1 and 2 were set to be 60 km and 50 km, respectively. The covariance matrices for the CEKF and MGEKF algorithms were initialised according to section 3 with $\sigma_r = 15\,\text{km}$ and $\sigma_v^2 = 0.02\,(\text{km/s})^2$. Note that $\sigma_v^2 = 0.02$ corresponds to a uniform speed assumption, with a maximum speed of 900 km/h. The initialisation of the covariance matrices for the MPEKF algorithm was done on an adhoc basis as the algorithm showed great sensitivity to initialisation parameters. Though no claim of optimality is implied, the Modified Polar coordinate EKF was found to perform well, when its covariance matrix was initialised according to

$$\begin{aligned} P(0|0) &= \text{diag}\,[7.2 \times 10^{-5}, 4 \times 10^{-6}, 9 \times 10^{-3}, 7 \times 10^{-10}], \quad \text{scenario 1} \\ P(0|0) &= \text{diag}\,[6 \times 10^{-3}, 3.6 \times 10^{-7}, 9 \times 10^{-3}, 1 \times 10^{-11}], \quad \text{scenario 2} \end{aligned}$$

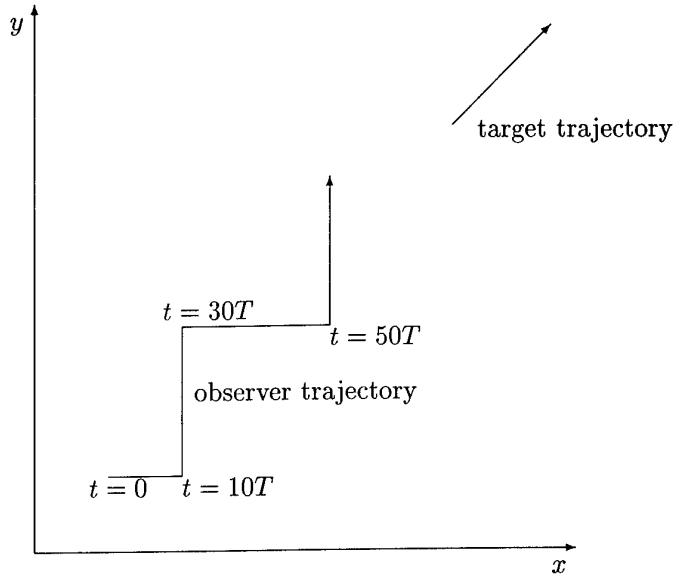

Figure 2: Target-Observer geometry for the simulations

Finally, all results have been ensemble averaged over 100 Monte-Carlo runs.

Figure 3 shows the estimation errors for range, azimuth, speed, and heading, corresponding to scenario 1 (initial range 35 km). From these results, we note that for the scenarios considered, the modified gain EKF only results in marginal improvements in the estimates compared with the standard Cartesian EKF. In fact, the MGEKF and CEKF show almost identical performance. In all algorithms, the range estimates converged to within about 5 km from the true range after 3 maneuvers. Also, note that the step-jump-like features of some of these error curves correspond roughly to the times at which ownship executes a maneuver. Azimuth estimate performances for all algorithms were good throughout the observation period except for PLE which shows erratic behaviour during the initial period. This is due to the fact that the PLE initialisation is scenario independent (zero initial state vector), and thus a large initial error is expected before a maneuver. For speed estimates, the results of Fig 3 show that CEKF and MGEKF were the best while PLE exhibits considerable bias. However, note that the heading error corresponding to the PLE and MPEKF converges quickly to zero compared with the other two algorithms.

Figure 4 shows similar results for scenario 2 where the initial range is 70 km. From these graphs it is evident that the MPEKF outperforms the other algorithms in terms of convergence of error in the quantities of interest. Also, though the azimuth and heading error estimates show comparable asymptotic performance in all four algorithms, the range and speed estimate errors have substantial bias in all but the Modified Polar coordinate EKF.

It must be emphasised that the performance of all the single-filter algorithms considered (except PLE) depends very much on the initialisation parameters for the state vector and

its covariance. Further, since the Cartesian and Modified Polar coordinate EKFs have different state vector and covariance matrices, its initialisation is also quite different. Thus, it is difficult to obtain a reliable comparison of the four single-filter tracking algorithms under an equivalent set of initialisation parameters. Nevertheless, the simulations such as the one carried out here should still highlight certain features pertinent to these algorithms, such as the biased estimates of PLE.

Next, we discuss the simulation results for the range-parameterised trackers, namely RPCEKF and RPMPEKF. For the use of RP trackers, the range interval (R_{min}, R_{max}) was chosen to be (5 km, 160 km). In addition, a 20% coefficient of variation for the range estimate was selected, which resulted in a division of the range interval into five subintervals, with subinterval boundaries $(5, 10, 20, 40, 80, 160)$ km. Thus, five EKF trackers were used for each RP tracker. The weighting threshold was set at 0.001 so that weights below this value implied the removal of the corresponding filter from the tracking process.

Figure 5 compares the estimation errors for CEKF and MPEKF with their corresponding RP counterparts for the case where initial target range is 70 km. The initial range estimate for the CEKF and MPEKF were selected such that the initial range error was 40 km. Furthermore, the MPEKF was initialised according to section 6.2, i.e., the initial covariance matrix was not 'tuned' for optimum performance. In Fig 5, the large initial fluctuations in estimation errors for the MPEKF algorithm show that this algorithm is rather sensitive to initialisation parameters. Also, a comparison of estimation errors shows that the corresponding RP trackers are better than CEKF and MPEKF, except for asymptotic heading error which was best for the CEKF. In addition, the results show that the two RP trackers, RPCEKF and RPMPEKF, exhibit similar performance. Although the RP trackers show good overall error performance, due to the large initial range errors, the speed estimates have substantial bias.

Figure 6 shows similar results to Fig 5 for the case where the MPEKF initial covariance matrix is optimised by trial and error. When the MPEKF algorithm is tuned this way, it is evident from Fig 6 that it outperforms the RP trackers. This, however, is not a very practical scheme as it involves a trial and error tuning of the initial covariance matrix. From Figs 5 and 6, it is seen that the MPEKF algorithm is very sensitive to initialisation parameters, particularly to the setting of the initial covariance matrix. The advantage of using the RP trackers is that they seem to perform well without a need to tune the initialisation parameters (as can be seen from Fig 5). This is the most attractive feature of the RP trackers.

Figure 7 shows similar results to Fig 5 for the case where the initial range error is 20 km. For this relatively small range error, Fig 7 shows that there is very little or no improvement in using the RP trackers instead of CEKF or MPEKF. Thus, we infer that the RP trackers are beneficial only when there is very little *a priori* knowledge of the initial range estimate.

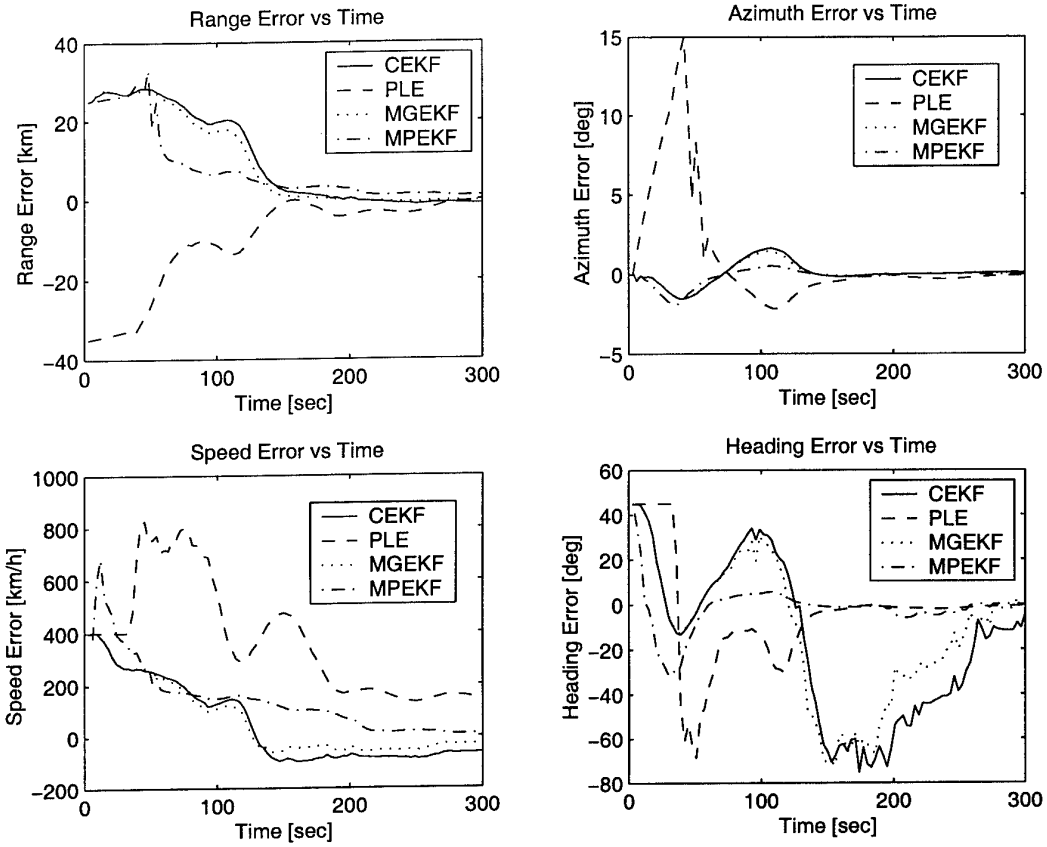

Figure 3: Track Estimation Errors for Scenario 1. Comparison of the four single-filter Angle-only TMA algorithms

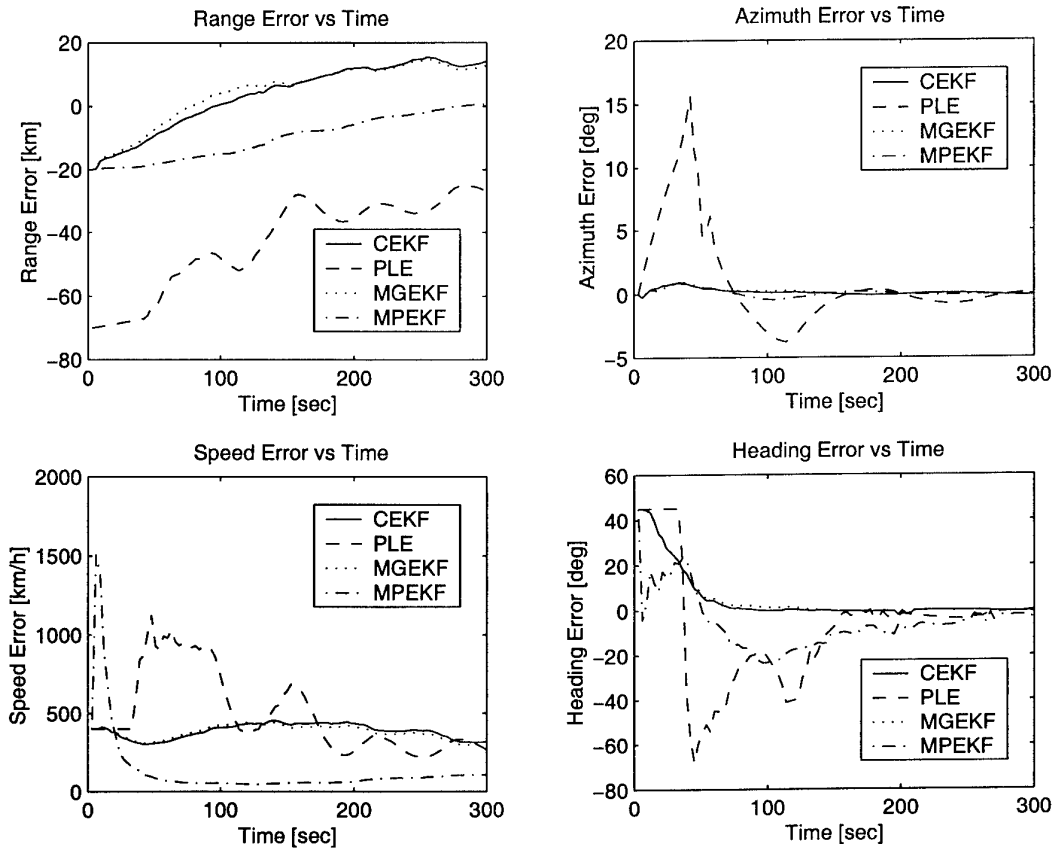

Figure 4: Track Estimation Errors for Scenario 2. Comparison of the four single-filter Angle-only TMA algorithms

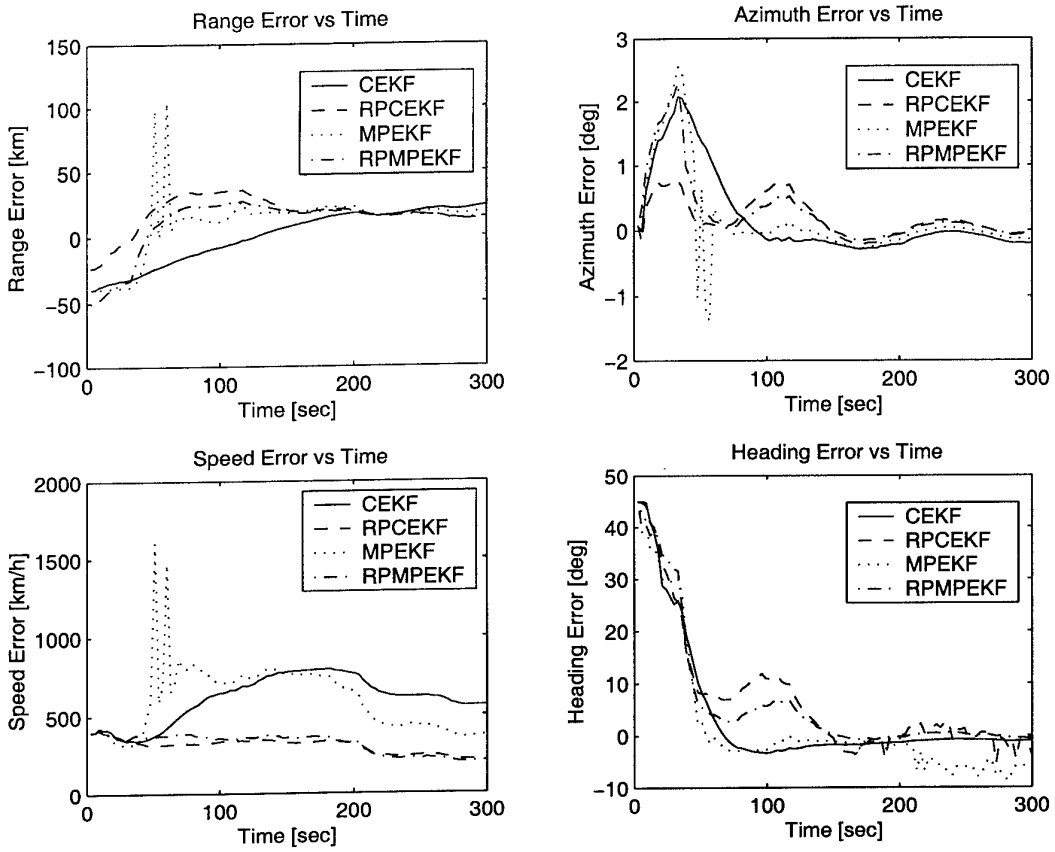

Figure 5: Comparison of the RP trackers with their single-filter counterparts. MPEKF tracker initialisation not optimised. Initial range error for the single-filter trackers 40 km

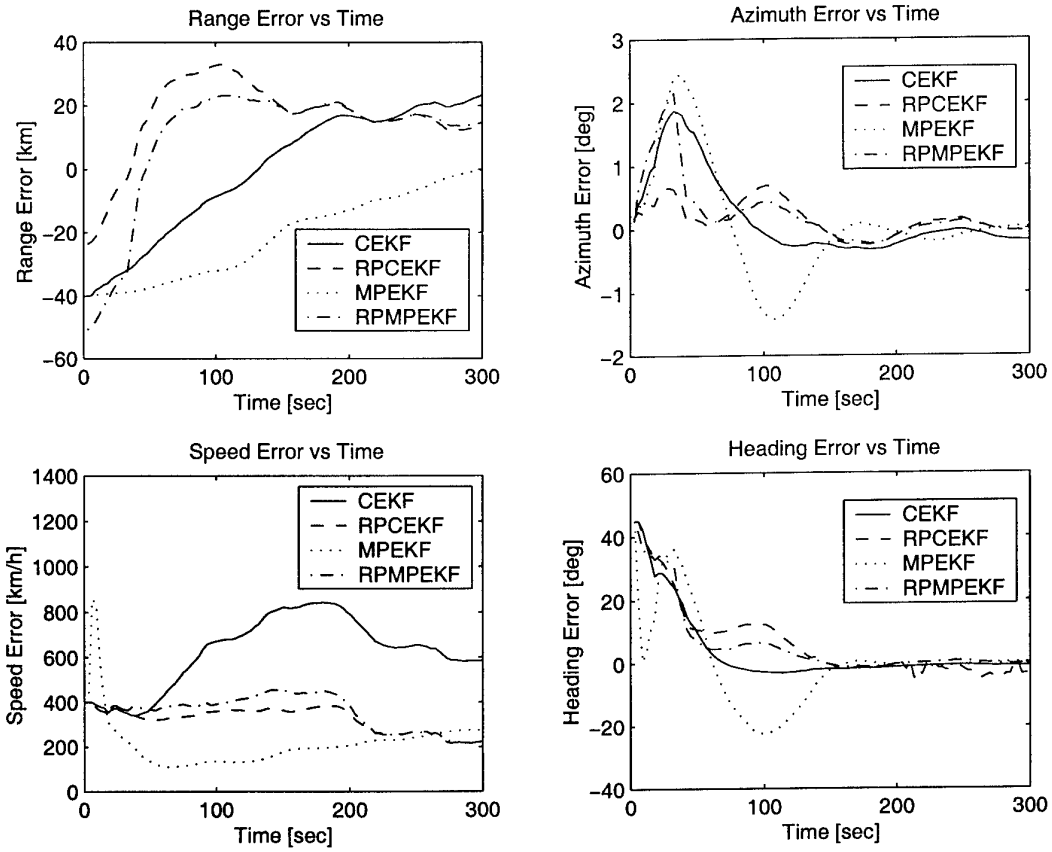

Figure 6: Comparison of the RP trackers with their single-filter counterparts. MPEKF tracker initialisation optimised by trial and error. Initial range error for the single-filter trackers 40 km

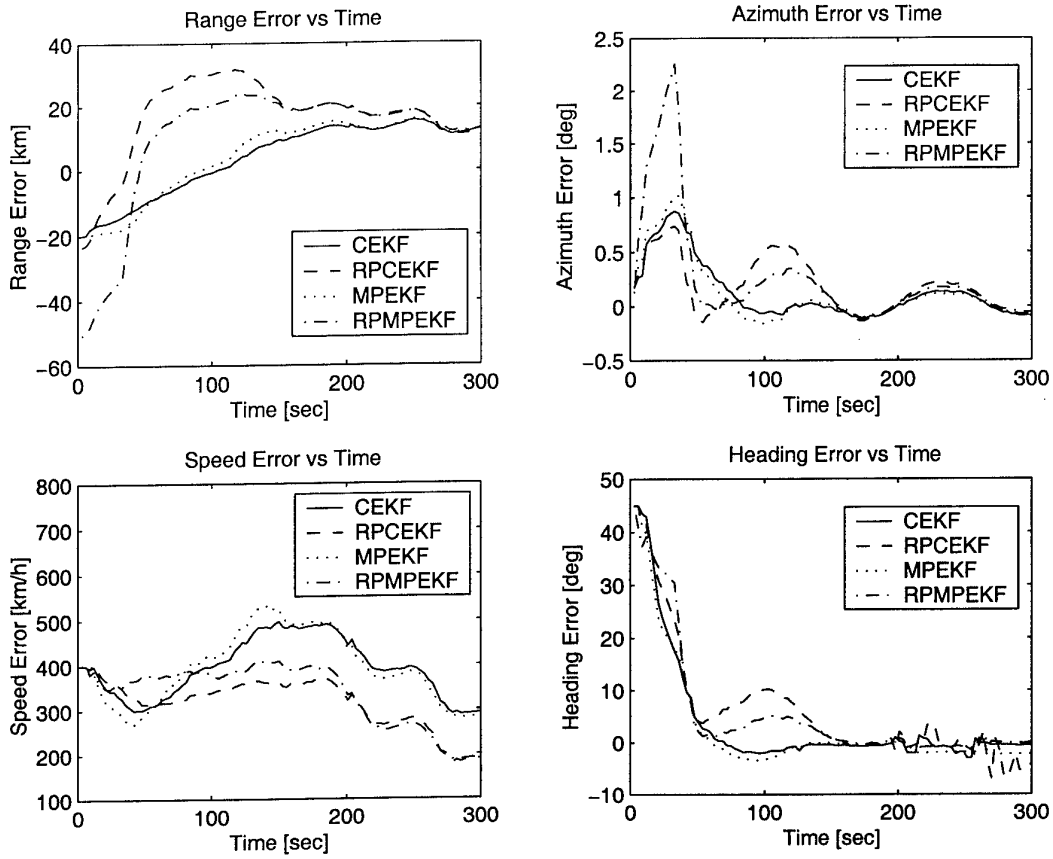

Figure 7: Comparison of the RP trackers with their single-filter counterparts. MPEKF tracker initialisation not optimised. Initial range error for the single-filter trackers 20 km

9 Conclusion and Further Work

This report has presented a survey of recursive style angle-only TMA algorithms that have potential application in airborne tracking in a jamming environment, particularly for estimation of the range to the jammer. The algorithms considered were, a) Cartesian coordinate EKF, b) Pseudo-Linear estimator, c) Modified gain EKF, d) Modified Polar coordinate EKF, e) Range-Parameterised Cartesian coordinate EKF, and f) Range-Parameterised Modified Polar coordinate EKF. The first four algorithms consist of single filters and the last two are based on a weighted sum of multiple filter outputs.

Among the single-filter trackers, the MPEKF appears to be slightly better for the scenarios considered. However, it is found that the MPEKF algorithm relies very much on proper initialisation parameters, particularly the initial state error covariance matrix, which in some cases needs tuning by trial and error. This initialisation problem is overcome by the range-parameterised trackers which produce good results even with virtually no *a priori* knowledge of initial target range. However, this advantage comes with an increased computational requirement due to the parallel processing of multiple filters. Further results show that if the initial range error for the single-filter trackers is small, then their performance is no worse than that of the RP trackers.

The next stage of the angle-only TMA research will address a number of issues. First, a systematic initialisation procedure based on [14] will be developed for the MPEKF algorithm to remove the current adhoc tuning of the initialisation parameters. Second, so far no attempt has been made to optimise observer trajectory for optimum performance, within the bounds of normal engagement maneuvers. Thus this needs to be investigated. Third, the case where angle information and ambiguous range and doppler information is available, such as in the case of multiple false target jamming and other deceptive jamming techniques, will be explored. Fourth, the difficult problem of angle-only target motion analysis for the case of a maneuvering target will be attacked. Though it has been recognised as a challenging problem, it deserves attention as the problem is very realistic. Next, the dimensionality will be increased from 2-D to 3-D to make these algorithms more suited for airborne applications. Finally, the developed algorithms will be incorporated into the existing pulse-doppler airborne radar model and tested against the simulated scenarios involving deceptive jamming.

Acknowledgements

The author wishes to sincerely thank his supervisor Dr Branko Ristic for introducing him to this interesting area of research, and for many valuable ideas and suggestions. The author also wishes to thank Dr John Whitrow, Head, Surveillance Sensor Processing, for kindly spending his time reviewing this report, and for providing constructive comments.

Appendix A: Computation of the linearised transition matrix

The linearised transition matrix F(k+1,k), for the Modified Polar coordinate EKF, was defined to be

$$F(k+1,k) = \left.\frac{\partial f\left[Y(k);k,k+1\right]}{\partial Y}\right|_{Y=\hat{Y}(k|k)} \tag{A1}$$

The RHS of (A1) can be written as [9]

$$\left.\frac{\partial f\left[Y(k);k,k+1\right]}{\partial Y}\right|_{Y=\hat{Y}(k|k)} = C + DE \tag{A2}$$

where

$$\begin{aligned} C &= [c_{ij}], \quad c_{ij} = \frac{\partial f_i}{\partial y_j}, \\ D &= [d_{ij}], \quad d_{ij} = \frac{\partial f_i}{\partial \alpha_j}, \\ E &= [e_{ij}], \quad e_{ij} = \frac{\partial \alpha_i}{\partial y_j}. \end{aligned} \tag{A3}$$

The elements c_{ij}, d_{ij} and e_{ij} can be evaluated with the result

$$C = \begin{bmatrix} 0 & 0 & 0 & 0 \\ 0 & 0 & 0 & 0 \\ 0 & 0 & 1 & 0 \\ 0 & 0 & 0 & 1/(\alpha_1^2+\alpha_2^2)^{1/2} \end{bmatrix} \tag{A4}$$

and

$$D = \begin{bmatrix} d_{11} & -d_{21} & d_{13} & d_{32} \\ d_{21} & d_{11} & -d_{32} & d_{13} \\ d_{31} & d_{32} & 0 & 0 \\ d_{41} & d_{42} & 0 & 0 \end{bmatrix} \tag{A5}$$

where

$$\begin{aligned} d_{11} &= \left[-\alpha_1(\alpha_2\alpha_3 - \alpha_1\alpha_4) - \alpha_2(\alpha_1\alpha_3 + \alpha_2\alpha_4)\right]/(\alpha_1^2+\alpha_2^2)^2 \\ d_{21} &= \left[-\alpha_1(\alpha_1\alpha_3 + \alpha_2\alpha_4) + \alpha_2(\alpha_2\alpha_3 - \alpha_1\alpha_4)\right]/(\alpha_1^2+\alpha_2^2)^2 \\ d_{31} &= \alpha_2/(\alpha_1^2+\alpha_2^2) \\ d_{41} &= -\alpha_1\hat{y}_4(k|k)/(\alpha_1^2+\alpha_2^2)^{3/2} \\ d_{32} &= -\alpha_1/(\alpha_1^2+\alpha_2^2) \\ d_{42} &= -\alpha_2\hat{y}_4(k|k)/(\alpha_1^2+\alpha_2^2)^{3/2} \\ d_{13} &= \alpha_2/(\alpha_1^2+\alpha_2^2) \end{aligned} \tag{A6}$$

and

$$E = \begin{bmatrix} T & 0 & e_{13} & e_{14} \\ 0 & T & e_{23} & e_{24} \\ 1 & 0 & e_{33} & e_{34} \\ 0 & 1 & e_{43} & e_{44} \end{bmatrix} \tag{A7}$$

where

$$
\begin{aligned}
e_{14} &= -\left[u_1(k,k+1)\cos\hat{y}_3(k|k) - u_2(k,k+1)\sin\hat{y}_3(k|k)\right] \\
e_{24} &= -\left[u_1(k,k+1)\sin\hat{y}_3(k|k) + u_2(k,k+1)\cos\hat{y}_3(k|k)\right] \\
e_{34} &= -\left[u_3(k,k+1)\cos\hat{y}_3(k|k) - u_4(k,k+1)\sin\hat{y}_3(k|k)\right] \\
e_{44} &= -\left[u_3(k,k+1)\sin\hat{y}_3(k|k) + u_4(k,k+1)\cos\hat{y}_3(k|k)\right] \\
e_{13} &= -\hat{y}_4(k|k)e_{24} \\
e_{23} &= \hat{y}_4(k|k)e_{14} \\
e_{33} &= -\hat{y}_4(k|k)e_{44} \\
e_{43} &= \hat{y}_4(k|k)e_{34}
\end{aligned}
\tag{A8}
$$

References

1. Lindgren A. G. and K. F. Gong, "Position and Velocity Estimation via Bearing Observations," *IEEE Trans. on Aerospace and Electronic Systems,* Vol. AES-14, pp. 564-577, July 1978.

2. Aidala, V. J., "Kalman Filter Behaviour in Bearings-only Tracking Applications," *IEEE Trans. on Aerospace and Electronic Systems,* AES-15, pp. 29-39, Jan. 1979.

3. Aidala, V. J. and S. C. Nardone, "Biased Estimation Properties of the Pseudo-linear Tracking filter," *IEEE Trans. on Aerospace and Electronic Systems,* Vol. AES-18, No. 4, pp. 432-441, July 1982.

4. Aidala, V. J. and S. E. Hammel, "Utilization of Modified Polar Coordinates for Bearings-only Tracking," *IEEE Trans. on Automatic control,* Vol. AC-28, No. 3, pp. 283-294, March 1983.

5. Nardone, S. C. and V. J. Aidala, "Observability Criteria for Bearings-only Target Motion Analysis," *IEEE Trans. on Aerospace and Electronic Systems,* Vol. AES-17, No. 2, pp. 162-166, March 1981.

6. Nardone, S. C., A. G. Lindgren, and K. F. Gong, "Fundamental Properties and Performance of Conventional Bearings-only Target Motion Analysis," *IEEE Trans. Automatic Control,* Vol. AC-29, No. 9, pp. 775-787, Sept. 1984.

7. Hammel, S. E. and V. J. Aidala, "Observability requirements for three dimensional Tracking via Angle Measurements," *IEEE Trans. on Aerospace and Electronic Systems,* Vol. AES-21, No. 2, pp. 200-207, March 1985.

8. Stallard, D. V., "An Angle-Only Tracking Filter in Modified Spherical Coordinates," *AIAA Guidance, Navigation, and Control Conference Proceedings,* Monterey, California, U.S.A, Paper 87-2380, pp. 542-550, 1987.

9. Hassab, J. C., "Underwater Signal and Data Processing," CRC Press, Boca Raton, Florida, 1989.

10. Song, T. A. and J. L. Speyer, "A stochastic Analysis of a Modified Gain Extended Kalman Filter with Application to Estimation with Bearings-only Measurements," *IEEE Trans. on Automatic Control,* Vol. AC-30, No. 10, pp. 940-949, Oct. 1985.

11. Galkowski, P. J. and M. A. Islam, "An Alternative Derivation of the Modified Gain Function of Song and Speyer," *IEEE Trans. on Automatic Control,* Vol. AC-36, No. 11, pp. 1323-1326, Nov. 1991.

12. Gordon, N. J., D. J. Salmond, and A. F. M. Smith, "Novel Approach to Nonlinear/Non-Gaussian Bayesian State Estimation," *IEE Proceedings-F,* Vol. 140, No. 2, pp. 107-113, April 1993.

13. Peach, N., "Bearings-only Tracking using a set of Range-Parameterised Extended Kalman Filters," *IEE Proc.-Control Theory Appl.,* Vol. 142, No. 1, pp. 73-80, Jan 1995.

14. Nardone, S. C. and M. L. Graham, "A Closed Form Solution to Bearings-Only Target Motion Analysis," *IEEE Journal of Oceanic Engineering,* Vol. 22, No. 1, pp. 168-178, Jan. 1997.

15. Kronhamn, T. R., "Bearings-only Target Motion Analysis Based on a Multihypothesis Kalman Filter and Adaptive Ownship Motion Control," *IEE Proc.-Radar, Sonar Navig.,* Vol. 145, No. 4, pp. 247-252, Aug 1998.

16. Oudjane, N. and C. Musso, "Regularised Particle Schemes Applied to the Tracking Problem," *Proceedings of the Internation Radar Symposium '98,* Vol. 1, pp. 1117-1126, Sept. 1998.

DISTRIBUTION LIST

A Comparison of Recursive Style Angle-only Target Motion Analysis Algorithms

Sanjeev Arulampalam

	Number of Copies
DEFENCE ORGANISATION	
Task Sponsor	
Gp Capt John Quaife, DACD	1
Gp Capt Clive Rossiter	1
S&T Program	
Chief Defence Scientist FAS Science Policy AS Science Corporate Management	1
Director General Science Policy Development	1
Counsellor, Defence Science, London	Doc Data Sht
Counsellor, Defence Science, Washington	Doc Data Sht
Scientific Adviser to MRDC, Thailand	Doc Data Sht
Scientific Adviser Policy and Command	1
Navy Scientific Adviser	Doc Data Sht
Scientific Adviser, Army	Doc Data Sht
Air Force Scientific Adviser	1
Director Trials	1
Aeronautical and Maritime Research Laboratory	
Director, Aeronautical and Maritime Research Laboratory	1
Chief, Weapons Systems Division	1
Chief, Maritime Operations Division	1
Dr Len Sciacca, HWSI	1
Dr Khusro Saleem	1
Electronics and Surveillance Research Laboratory	
Director, Electronics and Surveillance Research Laboratory	Doc Data Sht
Chief, Surveillance Systems Division	1
Chief, Electronic Warfare Division	1
Research Leader, Wide Area Surveillance	1
Research Leader, Surveillance for Air Superiority	1
Dr John Percival, HTSF	1
Dr John Whitrow, HSSP	1
Dr Branko Ristic	1

Author	3
DSTO Libraries	
Library Fishermans Bend	1
Library Maribyrnong	1
Library Salisbury	2
Australian Archives	1
Library, MOD, Pyrmont	Doc Data Sht
Library, MOD, Stirling	Doc Data Sht
Capability Development Division	
Director General Aerospace Development	1
Director General Maritime Development	Doc Data Sht
Director General Land Development	Doc Data Sht
Director General C3I Development	Doc Data Sht
Navy	
Army	
ABCA Standardisation Officer, Puckapunyal	4
NAPOC QWG Engineer NBCD c/- DENGRS-A, HQ Engineer Centre Liverpool Military Area, NSW 2174	Doc Data Sht
Air Force	
Intelligence Program	
DGSTA	1
Manager, Information Centre, Defence Intelligence Organisation	1
Acquisition Program	
Corporate Support Program (libraries)	
Officer in Charge, TRS, Defence Regional Library, Canberra	1
Officer in Charge, Document Exchange Centre	1
Additional copies for DEC for exchange agreements	
US Defense Technical Information Center	2
UK Defence Research Information Centre	2
Canada Defence Scientific Information Service	1
NZ Defence Information Centre	1
National Library of Australia	1
UNIVERSITIES AND COLLEGES	
Australian Defence Force Academy Library	1

Head of Aerospace and Mechanical Engineering, ADFA	1
Deakin University Library, Serials Section (M List)	1
Senior Librarian, Hargrave Library, Monash University	1
Librarian, Flinders University	1

OTHER ORGANISATIONS

NASA (Canberra)	1
Australian Government Publishing Service	1
The State Library of South Australia	1
Parliamentary Library of South Australia	1

ABSTRACTING AND INFORMATION ORGANISATIONS

Library, Chemical Abstracts Reference Service	1
Engineering Societies Library, US	1
Materials Information, Cambridge Science Abstracts, US	1
Documents Librarian, The Center for Research Libraries, US	1

INFORMATION EXCHANGE AGREEMENT PARTNERS

Acquisitions Unit, Science Reference and Information Service, UK	1
Library – Exchange Desk, National Institute of Standards and Technology, US	1
National Aerospace Library, Japan	1
National Aerospace Library, Netherlands	1

SPARES

DSTO Salisbury Research Library	5

Total number of copies:	65

DEFENCE SCIENCE AND TECHNOLOGY ORGANISATION DOCUMENT CONTROL DATA				1. CAVEAT/PRIVACY MARKING
2. TITLE A Comparison of Recursive Style Angle-only Target Motion Analysis Algorithms			3. SECURITY CLASSIFICATION Document (U) Title (U) Abstract (U)	
4. AUTHOR(S) Sanjeev Arulampalam			5. CORPORATE AUTHOR Electronics and Surveillance Research Laboratory PO Box 1500 Salisbury, South Australia, Australia 5108	
6a. DSTO NUMBER DSTO–TR–0917	6b. AR NUMBER AR-011-173		6c. TYPE OF REPORT Technical Report	7. DOCUMENT DATE January, 2000
8. FILE NUMBER	9. TASK NUMBER AIR 99/204	10. SPONSOR DACD	11. No OF PAGES 28	12. No OF REFS 16
13. DOWNGRADING / DELIMITING INSTRUCTIONS Not Applicable			14. RELEASE AUTHORITY Chief, Surveillance Systems Division	
15. SECONDARY RELEASE STATEMENT OF THIS DOCUMENT *Approved For Public Release* OVERSEAS ENQUIRIES OUTSIDE STATED LIMITATIONS SHOULD BE REFERRED THROUGH DOCUMENT EXCHANGE, PO BOX 1500, SALISBURY, SOUTH AUSTRALIA 5108				
16. DELIBERATE ANNOUNCEMENT No Limitations				
17. CITATION IN OTHER DOCUMENTS No Limitations				
18. DEFTEST DESCRIPTORS angle-only tracking jamming			EKF passive ranging	

19. ABSTRACT

This report presents a comparison of existing angle-only target motion analysis algorithms which have applications in tracking under jamming conditions. Though a number of different algorithms have been proposed for this problem, the particular emphasis in this report is recursive style algorithms which are more suited to airborne applications. In particular, six algorithms are considered, which are derivatives of either the standard or the extended Kalman filter. Four of these algorithms are single-filter trackers while the other two are based on weighted sum of multiple filter outputs. Simulation results are presented to verify the claimed properties of these algorithms